A SEMI-ANALYTICAL DISCRETIZATION METHOD FOR THE NEAR-FIELD ANALYSIS OF TWO-DIMENSIONAL MULTIMATERIAL WEDGES UNDER PLANE STRAIN CONDITIONS

Christian Mittelstedt*, Wilfried Becker**
[W. Becker]: becker@mechanik.tu-darmstadt.de
***AIRBUS Deutschland GmbH, Kreetslag 10, D-21129 Hamburg, Germany**
****Darmstadt University of Technology, Department of Mechanical Engineering, D-64289 Darmstadt, Germany**

Keywords: *Discretization Method, Multimaterial Junctions, Stress Singularities, Sectorial Elements, Semi-Analytical Method*

1 Introduction

Many engineering structures contain geometric discontinuities such as e.g. cracks, notches, cutouts and / or holes. Furthermore, especially when dealing with layered structures, material discontinuities such as interfaces between dissimilar materials are also encountered. Naturally, mixed forms of discontinuities often also occur, e.g. cracks in interfaces of composite laminates. Fig. 1 shows an example for an according structural situation which consists of a notched plate under some far field loading and which is composed of several dissimilar isotropic materials wherein the notch is characterized by the opening angle γ. The plate includes an arbitrary number of interfaces that share one common point of intersection at the tip of the notch where a cylindrical coordinate system x_1, r, φ and an orthonormal coordinate system x_1, x_2, x_3 are located.

It is well-known that the near-field state variables in the vicinity of the notch tip may be dominated by a stress singularity such that the stresses grow without bound when $r \to 0$. In such cases, a reasonable assumption for the displacements u_α and stresses $\sigma_{\alpha\beta}$ (α, β =1,2) may be found in the formulation as an infinite series where the displacements are postulated in the form $u \sim r^{\lambda}$:

$$u_\alpha(r,\varphi,\lambda) = \sum_{m=1}^{m=\infty} K_m r^{\lambda_m} g_{\alpha m}(\varphi), \qquad (1)$$

$$\sigma_{\alpha\beta}(r,\varphi,\lambda) = \sum_{m=1}^{m=\infty} K_m r^{\lambda_m - 1} f_{\alpha\beta m}(\varphi).$$

Therein, for the description of the angular variations of u_α and $\sigma_{\alpha\beta}$, the functions $g_{\alpha m}$ and $f_{\alpha\beta m}$ have been introduced. The quantity λ_m is most often denoted as eigenvalue, may be real or complex and depends on the near-field geometry and material data, while the generalized stress intensity factor K_m in addition is also governed by the far-field loadings and the structural situation in regions far from the local notch location. Obviously, when $\mathrm{Re}(\lambda_m) < 1$, the stresses become singular for $r \to 0$, while requirements for finite displacements and finite strain energy impose the restriction $\mathrm{Re}(\lambda_m) > 0$. Consequently, the quantity $\mathrm{Re}(\lambda_m) - 1$ is often referred to as *stress singularity exponent* or *order of the stress singularity*. The knowledge of λ_m is of importance since it may serve as an indicator for the potential criticality of a given structural situation with respect to local failure in the vicinity of a geometric and / or a material discontinuity.

The present investigation is devoted to the development and discussion of a novel semi-analytical method for the analysis of the orders of two-dimensional stress singularities $\mathrm{Re}(\lambda_m)$ - 1, $\mathrm{Im}(\lambda_m)$ as they typically occur in the near field of cracks and notches in junctions of an arbitrary number of isotropic linear elastic materials under plane strain conditions. For analysis purposes, this allows us to separate a circular section with the radius R from the overall structural situation as shown in fig. 1, middle portion. Speaking in terms of the cylindrical coordinate system x_1, r, φ, the method is based on a discretization of this circular section into an arbitrary number n of sectorial elements (fig. 1, middle portion) in which a simple linear interpolation scheme is employed with respect to φ

(fig. 1, lower portion) while postulating a set of unknown displacement functions in the mathematical interfaces between the elements which are dependent on the radial coordinate r only. This eventually allows for closed-form representations for both strains and stresses in each element k.

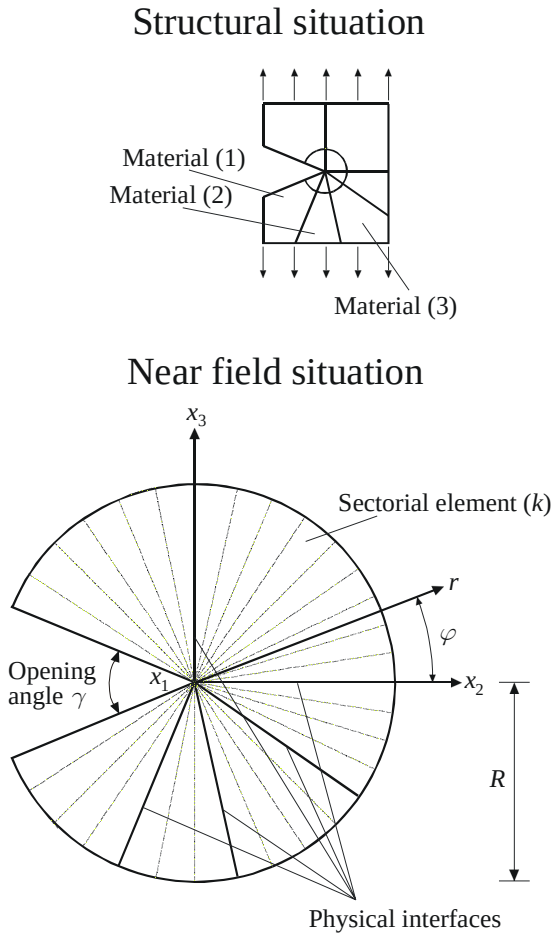

Fig. 1. Structural situation, discretization scheme, detail of a sectorial element.

The governing Euler-Lagrange equations that characterize the unknown displacement functions in the mathematical interfaces result from the principle of minimum elastic potential. Since this leads to differential equations of Euler-type, the governing equations can be solved in a closed-form analytical manner and the displacements result in formulations which suggest that $u \sim r^{\lambda}$. Therein, the exponent λ results from a quadratic eigenvalue problem that is encountered during the solution process of the governing Euler-Lagrange differential equations. This corresponds to the classical series expansion (1) so that the results of the present formulation can be straightforwardly interpreted as being the desired orders of the stress singularities in the vicinity of two-dimensional notch situations.

The near-field analysis of structural situations that contain geometric and / or material discontinuities has been the topic of a good number of scientific investigations during the last decades. An encompassing overview is beyond the scope of the present contribution so that only some representative works in this field are cited [1-7]. For selective overviews on this topic, the interested reader is referred to [8,9].

2 Displacement approach

In the sectorial element (k), the following approach for the radial and tangential displacement components u_r and u_φ is employed:

$$\begin{aligned} u_r^{(k)} &= U_r^{(k)}(r)\psi_1^{(k)}(\varphi) + U_r^{(k+1)}(r)\psi_2^{(k)}(\varphi), \\ u_\varphi^{(k)} &= U_\varphi^{(k)}(r)\psi_1^{(k)}(\varphi) + U_\varphi^{(k+1)}(r)\psi_2^{(k)}(\varphi). \end{aligned} \tag{2}$$

Therein, the unknown displacement functions U_r and U_φ are defined in the interfaces (k) and (k+1) of element (k), interrelated by the linear Lagrangian interpolation polynomials ψ_1 and ψ_2 (see fig. 1, lower portion). From this formulation, the strains within each element can be derived in a straightforward manner by the linearized strain-displacement relations (3), given in cylindrical coordinates:

$$\begin{aligned} \varepsilon_{rr}^{(k)} &= \frac{\partial u_r^{(k)}}{\partial r}, \quad \varepsilon_{\varphi\varphi}^{(k)} = \frac{1}{r}\left(\frac{\partial u_\varphi^{(k)}}{\partial \varphi} + u_r^{(k)}\right), \\ \gamma_{r\varphi}^{(k)} &= \frac{1}{r}\left(\frac{\partial u_r^{(k)}}{\partial \varphi} - u_\varphi^{(k)}\right) + \frac{\partial u_\varphi^{(k)}}{\partial r}. \end{aligned} \tag{3}$$

Hooke's law (4) eventually leads to the stress field in element (k):

$$\begin{pmatrix}\sigma_{rr}^{(k)}\\ \sigma_{\varphi\varphi}^{(k)}\\ \sigma_{11}^{(k)}\\ \sigma_{r\varphi}^{(k)}\end{pmatrix}=\begin{bmatrix}C_1^{(k)} & C_2^{(k)} & C_2^{(k)} & 0\\ C_2^{(k)} & C_1^{(k)} & C_2^{(k)} & 0\\ C_2^{(k)} & C_2^{(k)} & C_1^{(k)} & 0\\ 0 & 0 & 0 & C_3^{(k)}\end{bmatrix}\begin{pmatrix}\varepsilon_{rr}^{(k)}\\ \varepsilon_{\varphi\varphi}^{(k)}\\ \varepsilon_{11}^{(k)}\\ \gamma_{r\varphi}^{(k)}\end{pmatrix}. \qquad (4)$$

Therein, the stiffness components C_1, C_2 and C_3 for isotropic material behaviour can be written in terms of the modulus of elasticity E and the Poisson's ratio ν in the element (k) in a well-known manner as:

$$C_1^{(k)}=\frac{E^{(k)}\left(1-\nu^{(k)}\right)}{\left(1+\nu^{(k)}\right)\left(1-2\nu^{(k)}\right)},$$
$$C_2^{(k)}=\frac{E^{(k)}\nu^{(k)}}{\left(1+\nu^{(k)}\right)\left(1-2\nu^{(k)}\right)}, \qquad (5)$$
$$C_3^{(k)}=\frac{E^{(k)}}{2\left(1+\nu^{(k)}\right)}.$$

Note that in a state of plane strain, the stress components $\sigma_{\varphi 1}$ and σ_{1r} have to vanish.

3 Governing equations

The governing differential equations of the present problem which characterize the unknown displacement functions U_r and U_φ in the interfaces (k) and (k+1) of element (k) are derived from the principle of minimum elastic potential which in a contracted vector-matrix notation reads:

$$\Pi=\frac{1}{2}\sum_{m=1}^{m=n}\iiint_{V^{(m)}}\boldsymbol{\varepsilon}^{(m)^T}\boldsymbol{\sigma}^{(m)}dV^{(m)}=\text{Min.} \qquad (6)$$

Therein, all strains and stresses have been compiled in the one-dimensional arrays $\boldsymbol{\varepsilon}$ and $\boldsymbol{\sigma}$, respectively. Assuming that the considered plate has a unit thickness d = '1' and performing the integrations with respect to the circumferential coordinate φ, the underlying Euler-Lagrange-equations can be shown to read:

$$\frac{\partial F}{\partial U_r^{(k)}}-\frac{d}{dr}\left(\frac{\partial F}{\partial\left(\frac{\partial U_r^{(k)}}{\partial r}\right)}\right)=0,$$
$$\frac{\partial F}{\partial U_\varphi^{(k)}}-\frac{d}{dr}\left(\frac{\partial F}{\partial\left(\frac{\partial U_\varphi^{(k)}}{\partial r}\right)}\right)=0, \qquad (7)$$

wherein F is the integrand in (6). Evaluating (7) eventually leads to the following two coupled homogeneous Euler-type second-order differential equations, assembled over all interfaces:

$$\frac{1}{r}\mathbf{K}_1\mathbf{U}_r-\mathbf{K}_2\frac{\partial\mathbf{U}_r}{\partial r}-r\mathbf{K}_3\frac{\partial^2\mathbf{U}_r}{\partial r^2}$$
$$+\frac{1}{r}\mathbf{K}_4\mathbf{U}_\varphi+\mathbf{K}_5\frac{\partial\mathbf{U}_\varphi}{\partial r}=\mathbf{0},$$
$$\frac{1}{r}\mathbf{K}_6\mathbf{U}_r+\mathbf{K}_7\frac{\partial\mathbf{U}_r}{\partial r}+\frac{1}{r}\mathbf{K}_8\mathbf{U}_\varphi \qquad (8)$$
$$-\mathbf{K}_9\frac{\partial\mathbf{U}_\varphi}{\partial r}-r\mathbf{K}_{10}\frac{\partial^2\mathbf{U}_\varphi}{\partial r^2}=0.$$

The matrices $\mathbf{K}_1,\ldots,\mathbf{K}_{10}$ contain information about the geometric and material properties of the employed sectorial elements. For reasons of brevity, these quantities will not be discussed in more detail here. The arrays $\mathbf{U}_r$ and $\mathbf{U}_\varphi$ contain all displacement functions U_r and U_φ for all interfaces in a compiled manner. The equation system (8) can be adequately reformulated in a condensed form:

$$r\mathbf{H}_1\frac{\partial^2\mathbf{U}}{\partial r^2}+\mathbf{H}_2\frac{\partial\mathbf{U}}{\partial r}+\frac{1}{r}\mathbf{H}_3\mathbf{U}=\mathbf{0}. \qquad (9)$$

Therein, the vector $\mathbf{U}$ is the total displacement vector containing the arrays $\mathbf{U}_r$ and $\mathbf{U}_\varphi$ while the matrices $\mathbf{H}_1$, $\mathbf{H}_2$ and $\mathbf{H}_3$ include the original coefficient matrices $\mathbf{K}_1,\ldots,\mathbf{K}_{10}$.

4 Displacement solution

A solution approach can be sought in the form of power law functions as follows:

$$\mathbf{U}=\mathbf{A}r^\lambda. \qquad (10)$$

Inserting this solution approach into the governing equations (9), the terms r^λ cancel out and we eventually arrive at the following quadratic eigenvalue problem:

$$\left(\lambda^2\mathbf{H}_1+\lambda\left(\mathbf{H}_2-\mathbf{H}_1\right)+\mathbf{H}_3\right)\mathbf{A}=\mathbf{0}. \qquad (11)$$

This eigenvalue problem results in 2(n+1) eigenvalues λ and corresponding eigenvectors $\mathbf{A}$ so that a complete displacement solution $\mathbf{U}$ finally reads:

$$\mathbf{U}=\sum_{m=1}^{m=2(n+1)}b_m\mathbf{A}_m r^{\lambda_m}. \qquad (12)$$

It is worth noting that the resultant displacement solution **U** is of a functional form that enables a direct interpretation of the eigenvalues λ_m - 1 as the classical singularity exponents that characterize the stress singularities arising at notches and cracks in multimaterial interfaces (see eq. (1)).

5 Results and discussion

The presented analysis approach, even though being of a semi-analytical nature, consists of a one-dimensional discretization with respect to the circumferential coordinate φ. Hence, before discussing specific examples for the asymptotic study of the stress fields in the vicinity of multimaterial junctions, it is of basic interest to study the convergence properties of the derived analysis approach.

Müller et al. [7] presented results for the orders λ_m - 1 of stress singularities at bimaterial notches by using a complex potential approach. For the example of an interface crack between two isotropic materials with the ratio e of the Young's moduli $e = E_1/E_2 = 100$ and the Poisson's ratios given as $\nu_1 = \nu_2 = 0.2$, the order of the arising stress singularity was determined as the complex-conjugate value $\lambda_m - 1 = -0.5000 \pm 0.1227i$. Depending on the employed discretization scheme, the present methodology leads to practically the same results as tab. 1 shows:

Tab. 1: Results for the order λ - 1 of the stress singularity at the tip of an interface crack.

Number of elements	Order Re(λ - 1) of stress singularity	Order Im(λ - 1) of stress singularity
16	-0.4640	±0.1240
32	-0.4906	±0.1232
48	-0.4958	±0.1230
64	-0.4976	±0.1229
80	-0.4985	±0.1228
96	-0.4989	±0.1228
112	-0.4992	±0.1228
128	-0.4994	±0.1228

Obviously, only very little discretizational effort is needed to achieve results which match those of [7] very closely. This also becomes obvious when discussing the error evolution for Re(λ_m) – 1 and Im(λ_m) as given in fig. 2. A number of elements between 32 to 48 is needed for an accuracy of the results ensuring two correct significant digits which is a remarkable outcome when compared to standard finite element calculations which generally require thousands of degrees of freedom for this problem class. This demonstrates the excellent performance of the present method. With n = 96 elements, no variations in the third digit can be found so that this degree of discretization (which corresponds to n = 24 elements in each quadrant of the circular section) is employed for all further computations that are presented in this paper.

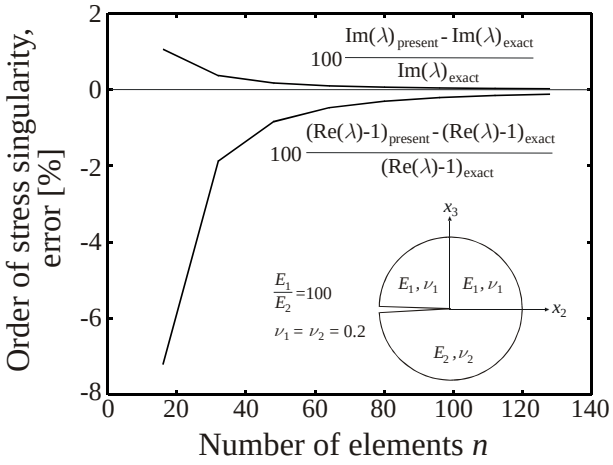

Fig. 2. Error evolution in the results for the order of the stress singularity Re(λ_m) - 1, Im(λ_m) at the tip of an interface crack between two isotropic materials.

The first example to be considered is a notch with an arbitrary opening angle γ which is located in the interface between two isotropic and linear elastic materials. Material 1 with the modulus of elasticity E_1 and the Poisson's ratio ν_1 is found in the range $x_3 \geq 0$ while material 2 (characterized by E_2 and ν_2) is located in the range $x_3 \leq 0$. Fig. 3 depicts the resultant orders Re(λ_m) - 1, Im(λ_m) of the occurring stress singularities for the notch opening angles $\gamma = 0°$, $\gamma = 30°$, $\gamma = 60°$, $\gamma = 90°$, $\gamma = 120°$ and $\gamma = 150°$ for a varying Poisson's ratio ν_2. Therein, the ratio $e = E_1/E_2$ of the Young's moduli was set to $e = 100$ while the Poisson's ratio ν_1 of material 1 was kept constant as $\nu_1 = 0.30$. As could be expected from engineering intuition, lower notch opening angles γ lead to stronger stress singularities since for a decreasing angle γ the situation of an interface crack is approached which, speaking very generally, is well-known to be associated with a high fracture criticality. For $\gamma = 0°$, we have Re(λ_m) – 1 = 0.5 which is a natural outcome for a stress singularity in the vicinity of a crack tip. A striking feature of the results contained in fig. 3 is the fact that for all $\gamma > 0°$, below some certain value of ν_2 the occurring

orders of the stress singularities are of a conjugate-complex nature so that the order of the stress singularity consists of a real part $\mathrm{Re}(\lambda_m) - 1$ (fig. 3, upper portion), and a non-vanishing imaginary part $\mathrm{Im}(\lambda_m)$ (see fig. 3, lower portion). For values of ν_2 above this specific threshold value, a bifurcation of the resultant orders of the stress singularities occurs and two purely real eigenvalues occur. Such bifurcation points which separate complex from purely real results are a common phenomenon when dealing with the near-field behaviour of stresses in the vicinity of multimaterial junctions and emphasize the rather complex nature of the presently considered problem class.

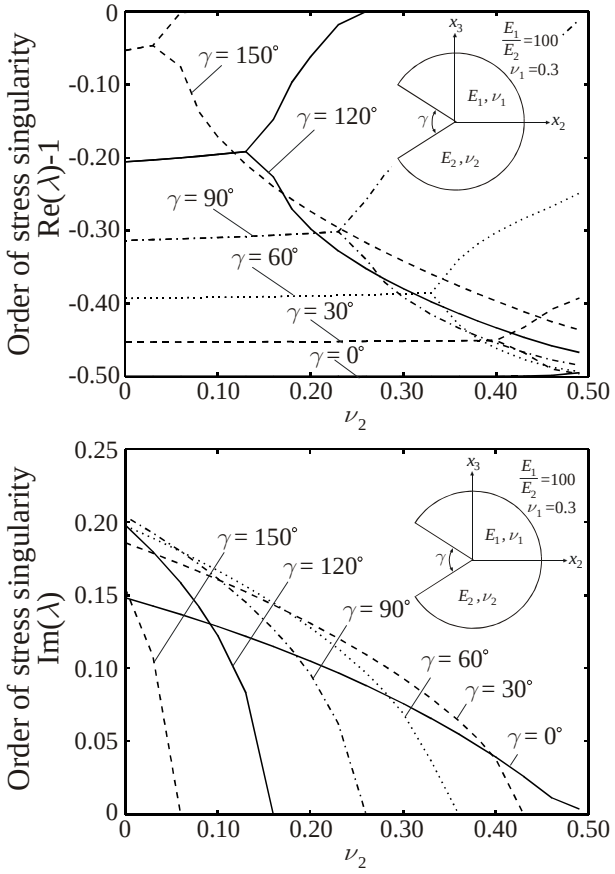

Fig. 3. Orders $\mathrm{Re}(\lambda_m)$ - 1, $\mathrm{Im}(\lambda_m)$ of the stress singularities at the vertices of notches with arbitrary opening angles γ between two isotropic materials.

The second example to be considered is a rectangular semi-infinite quarter-plane (material properties E_1 and ν_1) located in the range $x_2 \geq 0$, $x_3 \geq 0$ which is rigidly bonded to a semi-infinite half-plane (material properties E_2 and ν_2) located in the range $x_3 \leq 0$. Several values for the ratio $e = E_1/E_2$ of the Young's moduli were considered while the Poisson's ratio ν_1 was set to $\nu_1 = 0.30$. As before, results were generated for a varying Poisson's ratio ν_2 in the interval $0 \leq \nu_2 \leq 0.49$. Fig. 4 depicts the resultant orders of the occurring stress singularities for $e = 1$, $e = 21/16$, $e = 7/4$, $e = 14/5$, $e = 21/5$ and $e = 100$. Fig. 4, upper portion, shows the resultant real parts $\mathrm{Re}(\lambda_m) - 1$ while fig. 4, lower portion, depicts the according imaginary parts $\mathrm{Im}(\lambda_m)$. For all considered ratios e and Poisson's ratios ν_2, two purely real relevant eigenvalues occur wherein the dominating values are quite close to the classical crack-tip exponent $\mathrm{Re}(\lambda_m) - 1 = 0.5$ which emphasizes the possible fracture criticality of such bimaterial junction situations. An exception occurs for the ratio $e = 100$ where for long ranges of ν_2, the relevant eigenvalue is of a complex-conjugate nature which again highlights the quite complicated nature of the presently considered problem class.

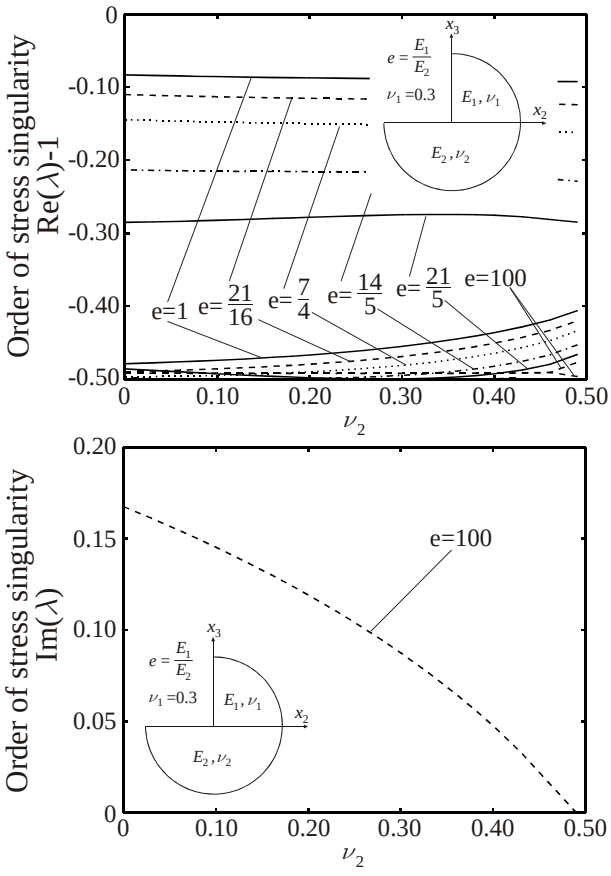

Fig. 4. Orders $\mathrm{Re}(\lambda_m)$ - 1, $\mathrm{Im}(\lambda_m)$ of the stress singularities at the tip of a bimaterial junction consisting of a semi-infinite quarter-plane (material 1) and a semi-infinite half-plane (material 2).

The third and last example deals with an interface crack in a bimaterial junction consisting of a semi-infinite quarter-plane (material 1) embedded in a

semi-infinite plane (material 2). The structural situation is given in fig. 5. The semi-infinite quarterplane (material properties E_1 and ν_1) is located in the range $x_2 \leq 0$, $x_3 \geq 0$, the semi-infinite half-plane (material properties E_2 and ν_2) occupies the region $x_2 \geq 0$, $x_3 \geq 0$ as well as $x_3 \leq 0$. The crack is located in the interface which runs parallel to the negative x_2-axis at $x_3 = 0$. Two exemplary sets of material properties were investigated wherein for both examples the Poissons's ratios were set to $\nu_1 = \nu_2 = 0.30$. In the first example, the ratio $e = E_1/E_2$ of the Young's moduli was assumed as $e = 1/100$ while in the second example, e was set to $e = 100$.

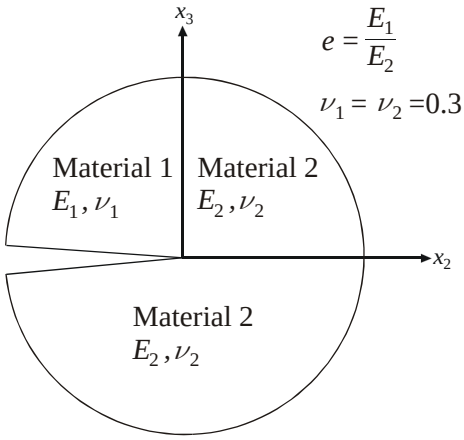

Fig. 5. Bimaterial junction consisting of a semi-infinite quarter-plane embedded in a semi-infinite plane with an interface crack in one of the interfaces.

Both examples reveal some interesting characteristics of the near-field behaviour of the state variables at the vertices of cracks and notches in multimaterial junctions which defy an ad-hoc explanation by simple engineering intuition alone. The first example leads to three purely real relevant eigenvalues that lead to singular stresses and which amount to $\lambda_1 - 1 = -0.0833$, $\lambda_2 - 1 = -0.2962$ and $\lambda_3 - 1 = -0.4552$. This is an unexpected result since, generally speaking, two-dimensional notch situations are usually associated with two relevant eigenvalues only. The second example leads to three relevant eigenvalues. Firstly, we have a purely real eigenvalue $\lambda_1 - 1 = -0.1240$. Secondly, a conjugate-complex eigenvalue with $\lambda_2 - 1 = -0.6504 + 0.0367i$ and $\lambda_3 - 1 = -0.6504 - 0.0367i$ occurs. Beside the occurrence of three relevant eigenvalues, we are confronted with the somewhat astonishing fact that the real parts of $\lambda_2 - 1$ and $\lambda_3 - 1$ distinctly exceed the classical two-dimensional crack tip singularitiy $\lambda - 1 = -0.5000$ which is typical for the singularities of the stresse field in the vicinity of cracks in homogeneous and isotropic materials and which as some kind of common engineering knowledge is often understood to be a general upper bound for the orders of stress singularities. Hence, speaking quite generally, especially the second example is associated with a rather high fracture criticality which should always be taken into account with care when dealing with the analysis of multimaterial junctions.

6 Summary and conclusions

We have presented a novel semi-analytical approach to the analysis of the near-field behaviour of displacements, strains and stresses in the vicinity of cracks and notches in multimaterial junctions consisting of an arbitrary number of dissimilar isotropic and linear-elastic materials. The method employs a discretization of the domain of interest into an arbitrary number of sectorial elements in each of which a linear interpolation with respect to the circumferential coordinate is used while in each of the mathematical interfaces between two elements, a priori unknown displacement functions are defined. These unknown displacement functions are determined from the principle of minimum elastic potential which leads to a set of governing Euler-Lagrange equations that can be solved in a closed-form analytical manner. The method works with high accuracy, however with a fraction of the computational effort that would have to be spent for according finite element calculations of comparable accuracy. This establishes the presented method as being highly reliable on the one hand while being very efficient on the other hand.

References

[1] Hein V.L. and Erdogan F. "Stress singularities in a two-material wedge". *International Journal of Fracture Mechanics*, Vol. 7, pp. 317-330, 1971.

[2] Kuo M.C. and Bogy D.B. "Plane solutions for the displacement and traction-displacement problems for anisotropic elastic wedges". *Journal of Applied Mechanics*, Vol. 41, pp. 197-202, 1974.

[3] Wang S.S. and Choi I. "Boundary-layer effects in composite laminates, part 1: free-edge stress singularities". *Journal of Applied Mechanics*, Vol. 49, pp. 541-548, 1982.

[4] Somaratna N. and Ting T.C.T. "Three-dimensional stress singularities in anisotropic materials and composites". *International Journal of Engineering Science*, Vol. 24, pp. 1115-1134, 1986.

[5] Ding S. and Kumosa M. “Singular stress behaviour at an adhesive interface corner”. *Engineering Fracture Mechanics*, Vol. 47, pp. 503-519, 1994.

[6] Pageau S.S., Joseph P.F. and Biggers S.B. “Finite element analysis of anisotropic materials with singular inplane stress fields”. *International Journal of Solids and Structures*, Vol. 32, pp. 571-591, 1995.

[7] Müller A., Hohe J. and Becker W. “A closed-form analysis of material and geometry effects on stress singularities at unsymmetric bimaterial notches”. *Proceedings in Applied Mathematics and Mechanics*, Vol. 2, pp. 210-211, 2003.

[8] Mittelstedt C. and Becker W. “Efficient computation of order and mode of three-dimensional stress singularities in linear elasticity by the boundary finite element method”.